

# Chemical and Morphological Evolution of PA-6/Epm/Epm-g-MA Blends in a Twin Screw Extruder

A. V. MACHADO,<sup>1</sup> J. A. COVAS,<sup>1</sup> M. VAN DUIN<sup>2</sup>

<sup>1</sup> Department of Polymer Engineering, University of Minho, 4800 Guimarães, Portugal

<sup>2</sup> DSM Research, P.O. Box 18, 6160 MD Geleen, The Netherlands

Received 17 June 1998; accepted 4 September 1998

**ABSTRACT:** Chemical conversion and morphological evolution of PA-6/EPM/EPM-g-MA blends along a twin screw extruder were monitored by quickly collecting small samples from the melt at specific barrel locations. The results show that the MA content of all blends decreases drastically in the first zone of the extruder, i.e., upon melting of the blend components. Significant changes in morphology are also observed at this stage. A correlation between chemistry and morphology could thus be established. © 1999 John Wiley & Sons, Inc. *J Polym Sci A: Polym Chem* 37: 1311–1320, 1999

**Keywords:** blend; chemical conversion; morphology; compatibilization

## INTRODUCTION

Polyamides (PAs) are extensively used in engineering applications due to their relatively high toughness and excellent chemical and abrasion resistance. However, toughness deteriorates significantly at low temperatures, thus preventing usage in specific applications. Blending PA with a small amount of a functional rubber has been shown to improve toughness. In fact, it has found widespread commercial application and has probably become one of the most studied examples of *in situ* compatibilization of polymer blends. Maleic anhydride (MA) modified styrene/ethylene/butylene/styrene block copolymers (SEBS-g-MA),<sup>1,2</sup> acrylonitrile/butadiene/styrene terpolymers (ABS) in combination with MA-containing compatibilizers,<sup>1–3</sup> emulsion-made core-shell rubbers (e.g., acrylic or butadiene-based rubber core and poly(methyl methacrylate) shell),<sup>4</sup> and MA-modified ethylene/propylene elastomers (EPM-g-MA)<sup>1,2,5–9</sup> have been successfully used for impact modification of PAs.

It was demonstrated that the MA grafted onto the rubber undergoes chemical reactions during melt blending with PA, the rubber's anhydride groups reacting with the polyamide's amine end groups to produce PA grafts on the rubber via imide linkages.<sup>1,5–8</sup> While noncompatibilized blends of PA-6/EPM exhibit a morphology with large dispersed particles without adhesion to the PA matrix, functionalized rubbers induce a very fine and stable dispersion of the rubber phase and act as an "interfacial agent" promoting adhesion between the matrix and the dispersed phase.<sup>1,5–7</sup> As for the effects of MA and of rubber concentration on the impact behavior of PA/rubbers blends, it is by now well-established that the brittle-ductile transition temperature shifts to lower values with increasing rubber concentration and decreasing particle size, and that the interfacial adhesion has no influence on that temperature.<sup>1,6</sup>

The above studies focussed on the extrudates produced upon melt blending. However, it is well known that the geometry of the mixing equipment and the operating conditions have a strong effect on the mixing intensity and quality. Consequently, the chemical conversion, the morphology and the rheology of the blends will be affected. It

Correspondence to: J. A. Covas

*Journal of Polymer Science: Part A: Polymer Chemistry*, Vol. 37, 1311–1320 (1999)  
© 1999 John Wiley & Sons, Inc. CCC 0887-624X/99/091311-10

**Table I.** Composition of the PA-6/EPM/EPM-*g*-MA Blends

| Blend       | EPM<br>(wt. %) | EPM- <i>g</i> -MA |                    | MA Content of the<br>Rubber Phase (wt. %) | MA Content of<br>the Blend (wt. %) |
|-------------|----------------|-------------------|--------------------|---|------------------------------------|
|             |                | (wt. %)           | MA Content (wt. %) |   |                                    |
| 80/20/0     | 20             | 0                 | 0                  | 0   | 0                                  |
| 80/15/5     | 15             | 5                 | 0.49               | 0.13                                      | 0.025                              |
| 80/10/10    | 10             | 10                | 0.49               | 0.25                                      | 0.049                              |
| 80/5/15     | 5              | 15                | 0.49               | 0.37                                      | 0.074                              |
| 80/0/20a    | 0              | 20                | 0.49               | 0.49                                      | 0.098                              |
| 80/0/20b    | 0              | 20                | 0.31               | 0.31                                      | 0.062                              |
| 80/11.5/8.5 | 11.5           | 8.5               | 0.47               | 0.20                                      | 0.040                              |
| 80/8/12     | 8              | 12                | 0.22               | 0.13                                      | 0.026                              |

should be realized that the processing of such reactive PA blends is of high complexity, since chemistry, morphology, and rheology continuously and mutually interact. Finally, the morphology and the interphase determine the physical/mechanical properties of the blends.<sup>1,8-11</sup>

Therefore, it is important to investigate how chemistry, rheology and morphology interact during the preparation of the blend. Surprisingly, there is little previous work on this area. Sundararaj et al.<sup>12</sup> published the first study of morphology changes along the length of a plasticating “clamshell” type twin screw extruder. They concluded that the major morphology changes occurred in the first kneading section; samples 20 mm further down the extruder exhibited a significant morphology evolution. However, sample collecting was relatively slow (the reported sampling times varied between 40 and 60 s), thus allowing for a significant relaxation of both matrix and dispersed polymer to occur after cessation of the shear. Later, the authors<sup>13</sup> showed that a high amount of interfacial area is generated very rapidly during melt mixing. This is important in the case of reactive blends, since it favors a high degree of interfacial reaction. Experimental observations related to recent efforts to speed up the material sampling procedure in order to produce more reliable samples<sup>14-16</sup> have confirmed the rapid development of morphology at the melting zone. As far as the evolution of chemical conversion along the extruder is concerned, Majumdar et al.,<sup>3</sup> again using a “clamshell” type extruder, recently reported that the degree of chemical conversion of some PA-based blends reaches a plateau in the initial regions of the screw and that the extent of the reaction varies with screw speed. A correlation between the extent of the reaction

and the particle size of the dispersed phase could be established.

The present work aims at studying the evolution of the chemical reaction of PA-6/EPM/EPM-*g*-MA blends in a twin screw extruder and how this correlates with the development and stability of the morphology along the screw length. For this purpose, small amounts of material were collected quickly at relevant locations from inside an extruder working under steady state conditions using a recently developed sampling device,<sup>16</sup> and quenched for subsequent characterization. The effect of changes of the blend composition was also studied.

## EXPERIMENTAL

### Materials

Commercial PA-6 (Akulon K123) and EPM (Keltan 740) produced by DSM, The Netherlands, were used. EPM-*g*-MA (Exxelor VA 1801, 1803, 1820, and 1810, containing 0.49, 0.47, 0.31 and 0.22 wt.% of MA, respectively, as determined by FT-IR) were kindly provided by Exxon, Spain. The amount of PA-6 was kept constant in all blends (80 wt.%), whereas the concentration of EPM and EPM-*g*-MA was varied as shown in Table I.

### Preparation of the Blends

The blends were prepared in a laboratory modular Leistritz LSM 30.34 intermeshing corotating twin-screw extruder coupled to the relevant downstream accessories. Blends were compounded with the screws rotating at 200 rpm,

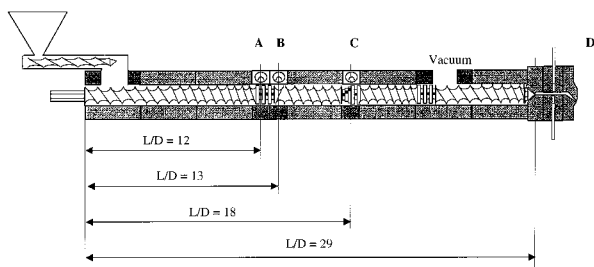


**Figure 1.** Screw configuration and sampling locations.

with a flow rate of 6 kg/h and set temperatures of 220–230°C in the barrel and 220°C at the die. Both the configuration of the screws and the axial location of the sampling devices (see Ref. 16 for a more complete description of these tools) are depicted in Figure 1. The material was collected at zones where the melt was being subjected to more intensive mixing and significant changes in morphology and/or chemistry would be anticipated, i.e. at staggering kneading blocks and at left-handed screw elements. Immediately after collection the samples were quenched in liquid nitrogen in order to prevent further reaction or coalescence.

### Characterization of Materials

The details of the chemical characterization of the PA blends are discussed elsewhere.<sup>10</sup> The samples were initially milled and dried overnight. Then, part of the samples was stirred in formic acid at room temperature during 24 h in order to extract all free PA-6. The nitrogen content of the centrifuged residues was determined with a LECO FP-428 nitrogen analyzer. The remaining of the samples was hydrolyzed with hydrochloric acid for 6 h and subsequently filtered, washed with water, and dried for 1 h at 180°C, in order to convert dicarboxylic acid back to anhydride. Thin films were prepared by compression-moulding and characterized by FT-IR (Perkin-Elmer 1720 spectrometer). The anhydride carbonyl peak at 1785  $\text{cm}^{-1}$  (see Fig. 2a), together with an IR calibration formula obtained with a set of references, allowed the quantitative determination of the MA content in the hydrochloric acid residues.

After fracture of the samples in liquid nitrogen, etching with boiling xylene to remove the rubber from the surface and gold plating, the morphology of the blends was studied using a Jeol JSM 6310F scanning electron microscope. Samples were

trimmed (in  $0.1 \times 0.2$  mm bits) at room temperature and stained with a 50/50 osmium tetroxide/formaldehyde mixture. Cryo-coups of about 70 nm thickness were cut at  $-100^\circ\text{C}$  and then analyzed with a Philips EM420 transmission electron microscope at 120 kV. The morphology was characterized in terms of the size and the size distribution of the dispersed phase. A Leica Quantimet 550 image analysis system was used to quantify the equivalent circle diameters, which were computed from individual particle areas, whereas the distribution width was estimated from the variance. At least 300 particles for each micrograph were observed for this purpose.

The thermal characterization of the blends was carried out in a power compensated Perkin Elmer DSC7. Circa 6–10 mg of each sample was scanned in the range 25–220°C at 10°C/min.

### RESULTS AND DISCUSSION

The sampling locations A to D are specified in Figure 1. They were chosen in order to follow the reactive blending process in real time. While A and C correspond to modules of kneading blocks in the screw, B is adjacent to a left-handed screw section. In all cases, high pressure and shear are developed, providing conditions for chemical reaction and/or droplet break-up. The collection of samples from conveying zones was avoided, since one anticipates that coalescence of the disperse phase will take place. Location D corresponds to the die exit (i.e., the extrudate).

The actual occurrence of a reaction between PA-6 and the MA modified rubber under the processing conditions selected was initially investigated. Figure 2 shows the FT-IR spectra of the 80/0/20a (w/w/w) blend at location A after hydrolysis with hydrochloric acid removing all aminocaproic acid units but not the one attached to EPM-g-MA (Fig. 2a) and of the initial EPM-g-MA (Fig. 2b). A comparison of these two spectra evidences the strong reduction of the peak intensity at 1785  $\text{cm}^{-1}$  upon blending, which implies that almost all anhydride groups have reacted. Moreover, the observation of a new peak at 1720  $\text{cm}^{-1}$  due to an imide group confirms the reaction between the MA modified rubber and the PA-6 in the blend, yielding a PA-EPM graft copolymer.<sup>1</sup>

Table II shows the residual MA content of EPM-g-MA for the various blends along the extruder, as determined by FT-IR. The MA content of the 80/0/20a blend, i.e., containing the largest

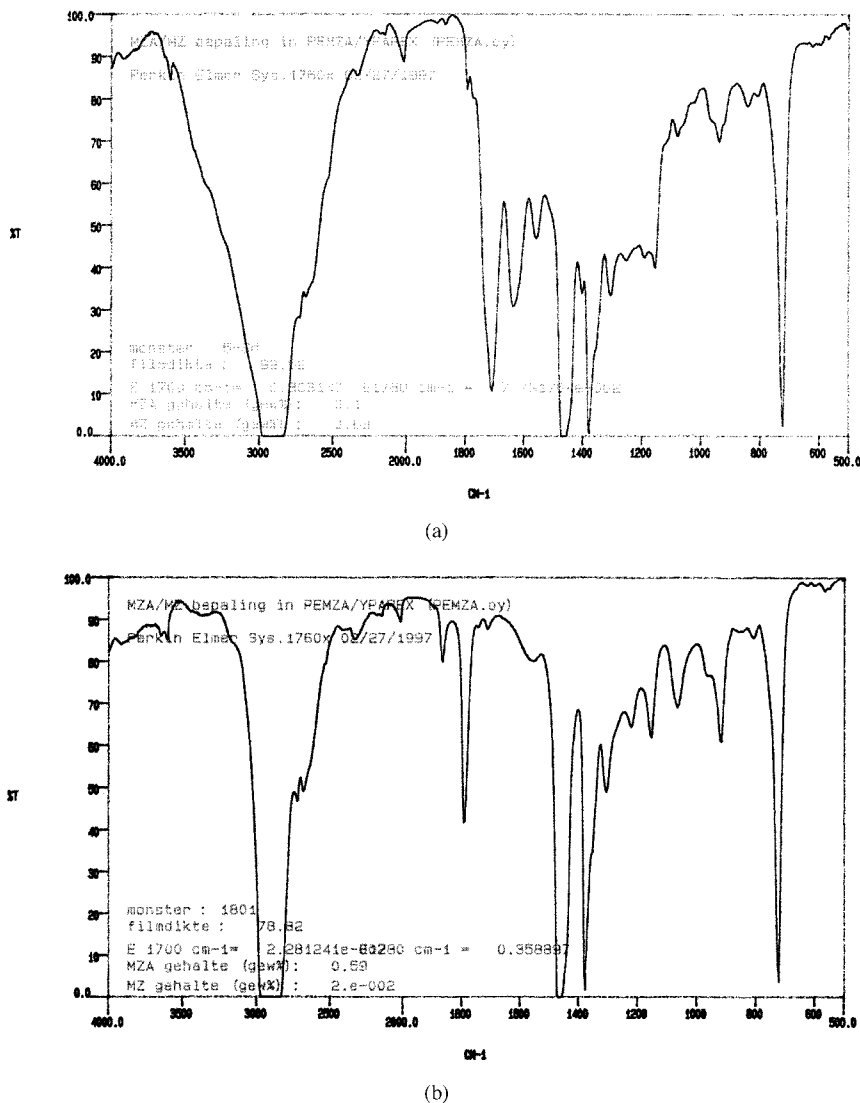


**Figure 2.** Infra-red spectra of (a) PA-6/EPM-g-MA (80/0/20a w/w/w) blend after hydrolysis with hydrochloric acid and (b) EPM-g-MA before blending.

amount of MA, decreased significantly from its original value in location A (0.49→0.07) and remains unchanged thereafter. As for the other blends with less MA, the ratio between the initial and the residual MA content is similar (0.13→0.02 for blend 80/15/5; 0.25→0.03 for blend 80/10/10; 0.37→0.06 for blend 80/5/15); the value at location A is already very small, and it was considered sufficient to present data only for locations A and D. The results indicate that for all blend compositions the MA content decreases drastically in the first part of the extruder up to the first kneading zone (location A), i.e., upon melting of the material, as will be seen later. Since almost all MA has reacted, an additional

decrease further on the extruder is not possible. This conclusion is in line with that of Scott,<sup>17</sup> who monitored this reaction in a batch mixer and reported a very fast reaction. The residual MA groups are probably located inside the rubber particles and not at the interface. This residual MA content along the extruder seems to be largely independent of the original MA content.

Both the amount of PA grafted during blending and the molecular weight of these grafts were computed from the nitrogen content of the residues, obtained after extraction of all free PA-6 from the blends and from the residual MA content, respectively (Table II). Within the experimental error, the PA graft content is independent

**Table II.** Chemical Conversion of PA-6/EPM/EPM-*g*-MA Blends as a Function of the Screw Length

| Blend       | Sampling Location | Residual MA Content of EPM- <i>g</i> -MA (Wt. %) | Reacted MA (%) | <i>N</i> (%) | PA-6 Grafted on 20 g of EPM + EPM- <i>g</i> -MA (g) | $\bar{M}_n$ of Grafted PA-6 (g/mol) |
|-------------|-------------------|--|----------------|--------------|---|-------------------------------------|
| 80/15/5     | A                 | 0.02   | 85             | 0.14         | 0.22  | 1000                                |
|             | D                 | 0  | 100            | 0.23         | 0.38  | 1400                                |
| 80/10/10    | A                 | 0.03   | 88             | 0.50         | 0.84  | 1900                                |
|             | D                 | 0.01   | 96             | 0.48         | 0.81  | 1700                                |
| 80/5/15     | A                 | 0.06   | 84             | 0.39         | 0.65  | 1000                                |
|             | D                 | 0.04   | 89             | 0.48         | 0.81  | 1200                                |
| 80/0/20a    | A                 | 0.07   | 86             | 0.45         | 0.75  | 900                                 |
|             | B                 | 0.07   | 86             | —            | —   | —                                   |
|             | C                 | 0.08   | 84             | 0.51         | 0.86  | 1000                                |
|             | D                 | 0.07   | 86             | 0.48         | 0.81  | 1000                                |
| 80/0/20b    | A                 | 0.07   | 68             | —            | —   | —                                   |
|             | D                 | 0.04   | 82             | —            | —   | —                                   |
| 80/11.5/8.5 | A                 | 0.03   | 85             | —            | —   | —                                   |
|             | D                 | 0.02   | 90             | —            | —   | —                                   |
| 80/8/12     | A                 | 0.05   | 75             | —            | —   | —                                   |
|             | D                 | 0.03   | 84             | —            | —   | —                                   |

of the sampling location, which is in agreement with the FT-IR observation that most MA is converted in location A. As the original MA content of the blends increases, the amount of PA grafted at the interface increases until it reaches a constant level of 0.8 g / 20 g EPM + EPM-*g*-MA. Parallely, the molecular weight of the grafted PA increases with increasing blend MA content. In summary, the number of chains grafted increases, and reaches a plateau, so their length decreases. Similar observations were reported by Duin et al.<sup>10</sup> and are related to the degradation of the PA chains grafted onto the modified rubber. When there is an excess of MA the degraded grafted PA chains will form new grafts, due to the reaction of amine groups formed from the amide bonds broken with MA groups of the rubber.

Since it has already been shown<sup>10</sup> that the degradation of PA can occur due to the effect of water formed as a product of the imide reaction during blending of PA and MA containing polymers, this was not pursued in this work. Degradation of PA can occur especially when the amount of MA is equal to or larger than the amount of PA end groups. Duin et al.<sup>10</sup> showed that for a SMA/PA-6 blend the molecular weight of the PA was about 0.05 of that of the original PA, i.e. 20 amide bonds of each PA chain were broken. This is not just thermal degradation, but a process which occurs in the presence of anhydrides only. Now, the reaction between anhydride

and amide towards imide can not be a direct one, since a molecule of water is missing in the reaction equation. This molecule of water may come from the water molecule released upon reaction of amine with anhydride to imide. Although the actual mechanism has not been proven, it is thought that there is a reaction cycle: first anhydride plus amine gives imide and water, then amide plus water gives amine etc. This is not surprising, since the solubility of water in PA-6 is very high and the equilibrium acid + amine  $\leftrightarrow$  amide + water is shifted to the left at higher temperatures. Finally, although the extruder is vented at the end, there will be sufficient pressure at other parts of the extruder to prevent water from devolatilizing.

Figures 3–5 show the evolution of the morphology of blends 80/20/0, 80/15/5, and 80/0/20a along the extruder, as observed by SEM after extraction of the rubber and by TEM for blend 80/0/20a, which has the highest MA content and exhibits a finer morphology. Figures 3a and 4a clearly show the presence of a solid PA pellet at location A surrounded by molten polyamide and rubber, which has the lowest  $T_g$  ( $-30^\circ\text{C}$ ). At location B (Figs. 3b and 4b), which is 4 cm downstream (see Fig. 1), the solid pellets are no longer present, only dispersed domains a few microns in size can be observed. These domains correspond to the rubber phase which was, as referred previously, extracted with hot xylene. Therefore, one can pos-

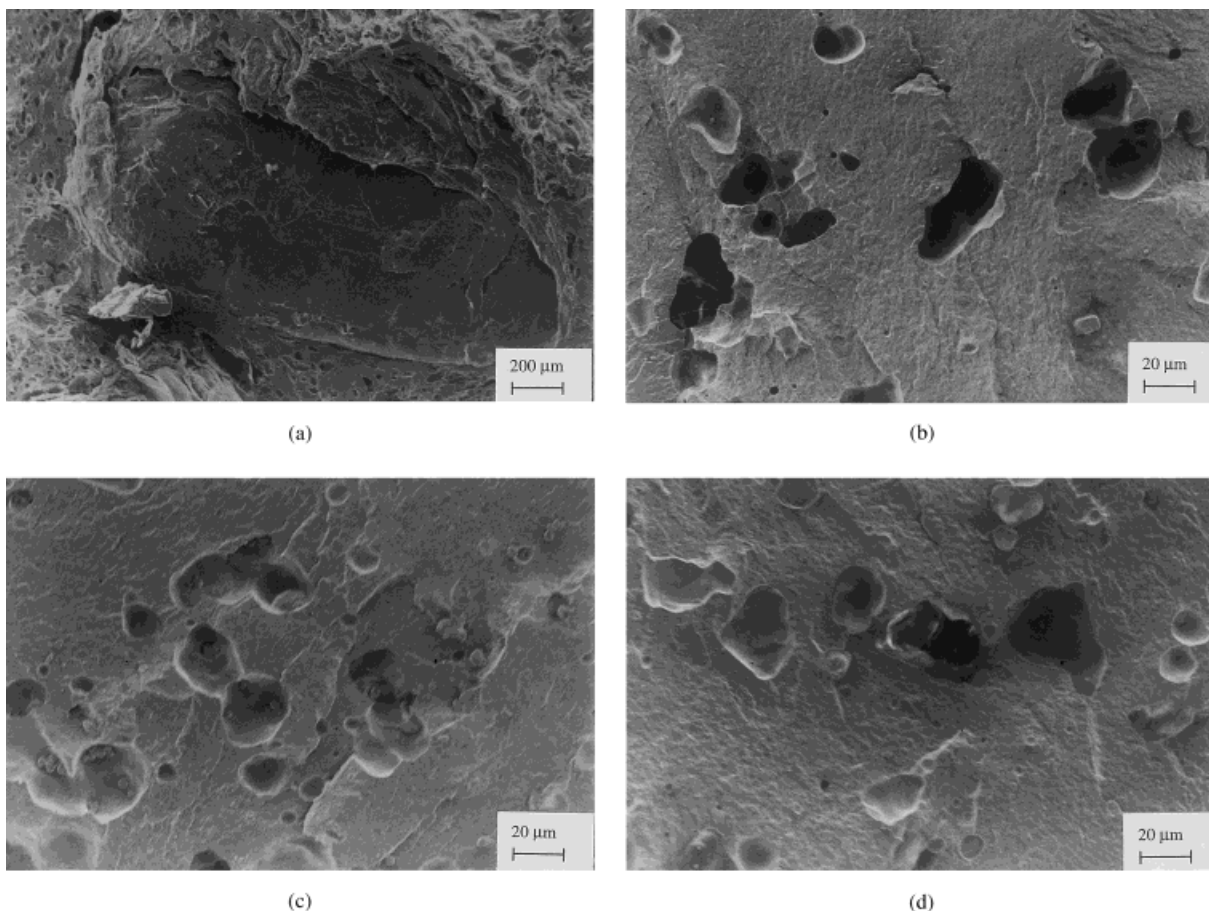


**Figure 3.** SEM micrographs of uncompatibilized PA-6/EPM (80/20 w/w) blend collected along the extruder at locations A to D (a, b, c, and d, respectively).

tulate that initially the rubber becomes the continuous phase, surrounding the solid PA-6 pellets. Upon melting of the PA-6 phase inversion will take place, i.e., rubber will constitute the dispersed phase. The observed occlusions in the rubber particles (Fig. 5) support this hypothesis. Clear evidence of this process is difficult to obtain, as changes in processing conditions did not alter significantly the rate of evolution of the morphology. If a high amount of interfacial area was already generated very rapidly upon melting, the phase inversion process may produce a further increase and, consequently, contribute to higher rates of conversion at this stage.

The dimensional characterization of the dispersed rubber particles is presented in Table III. Data for location A was not obtained, since PA is still partially unmelted and each specific blend was not yet produced. The nonreactive PA/EPM blend (Fig. 3) exhibits a rather large average particle size and no visible interfacial adhesion. Al-

though the particle size decreases along the extruder, the most significant changes in morphology occur during and immediately after melting. This type of behavior was previously observed by Sundararaj et al.,<sup>12</sup> who also suggested that a high amount of interfacial area is generated very rapidly,<sup>13</sup> thus favoring a high degree of interfacial reaction in the case of reactive blends. For the 80/5/15 blend (Table III and Fig. 4) the average rubber particle size is essentially constant (about 2.5  $\mu\text{m}$ ), but the particle size distribution significantly narrows. The same type of evolution was observed with the 80/0/20a blend. The material that had already melted at location A shows an irregular morphology with both spherical particles and ribbons or threads (Fig. 5a), whereas toward the die (Fig. 5b–d, respectively) fine regular spherical particles can be noticed. When the EPM-*g*-MA content of the blends is increased from 0 to 5 wt.% there is a strong decrease in particle size (distribution) due to in-situ compati-

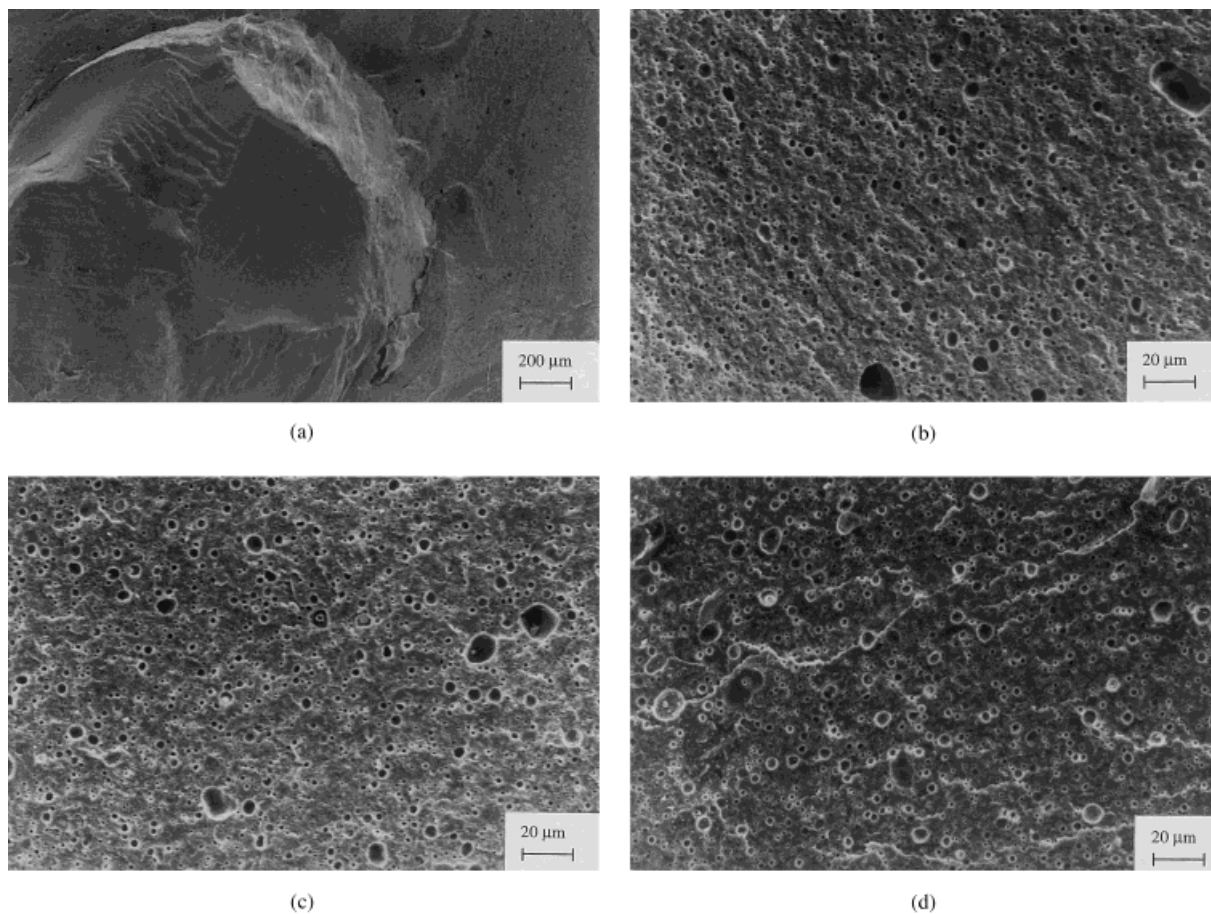


**Figure 4.** SEM micrographs of PA-6/EPM/EPM-*g*-MA (80/15/5 w/w/w) collected along the extruder at locations A to D (a, b, c, and d, respectively).

bilization. A further increase in EPM-*g*-MA content from 5 to 15 wt.% does not affect the particle size ( $2.7 \rightarrow 2.4 \rightarrow 2.3 \mu\text{m}$ ), but does result in a narrower distribution ( $6.5 \rightarrow 1.2 \rightarrow 0.7 \mu\text{m}^2$ ). However, a step change occurs when only EPM-*g*-MA is used and no non-functionalized EPM is added to the blend (80/0/20a). The particle size decreases to about  $0.3 \mu\text{m}$  and the distribution further narrows. This step change is probably due to the fact that all rubber chains are now converted into graft copolymers and for enthalpic reasons are driven to the interface. A strong increase in interfacial area, and thus a strong reduction in particle size, is needed to allow this.

The above results indicate the existence of a correlation between melting of the blend components, the conversion of the grafting reaction and the evolution of the morphology of the reactive blend. Major changes on morphology development are associated with high rates of chemical conversion. As seen above, the major morphology devel-

opment occurs in the first part of the extruder, where a high amount of interfacial area is generated. On the other hand, it is well known that the reaction between anhydride and aliphatic amine is one of the fastest.<sup>18</sup> Thus, interfacial area and reactivity are intrinsically associated for these systems. Since the intensive mechanical mixing after melting created by the staggered kneading blocks will not induce significant changes in morphology and, therefore, in chemical conversion (see Tables II and III), the graft copolymers formed upstream at the interface seem to provide sufficient steric stabilization against coalescence of the dispersed phase particles further down the extruder. Conversely, nonreactive blends are more sensitive to the intensity of mixing and to the thermal history.

The data also demonstrates that most of the chemical reaction occurs at the surface of the PA-6 pellets during the melting stage. The reaction between EPM-*g*-MA and PA proceeds already

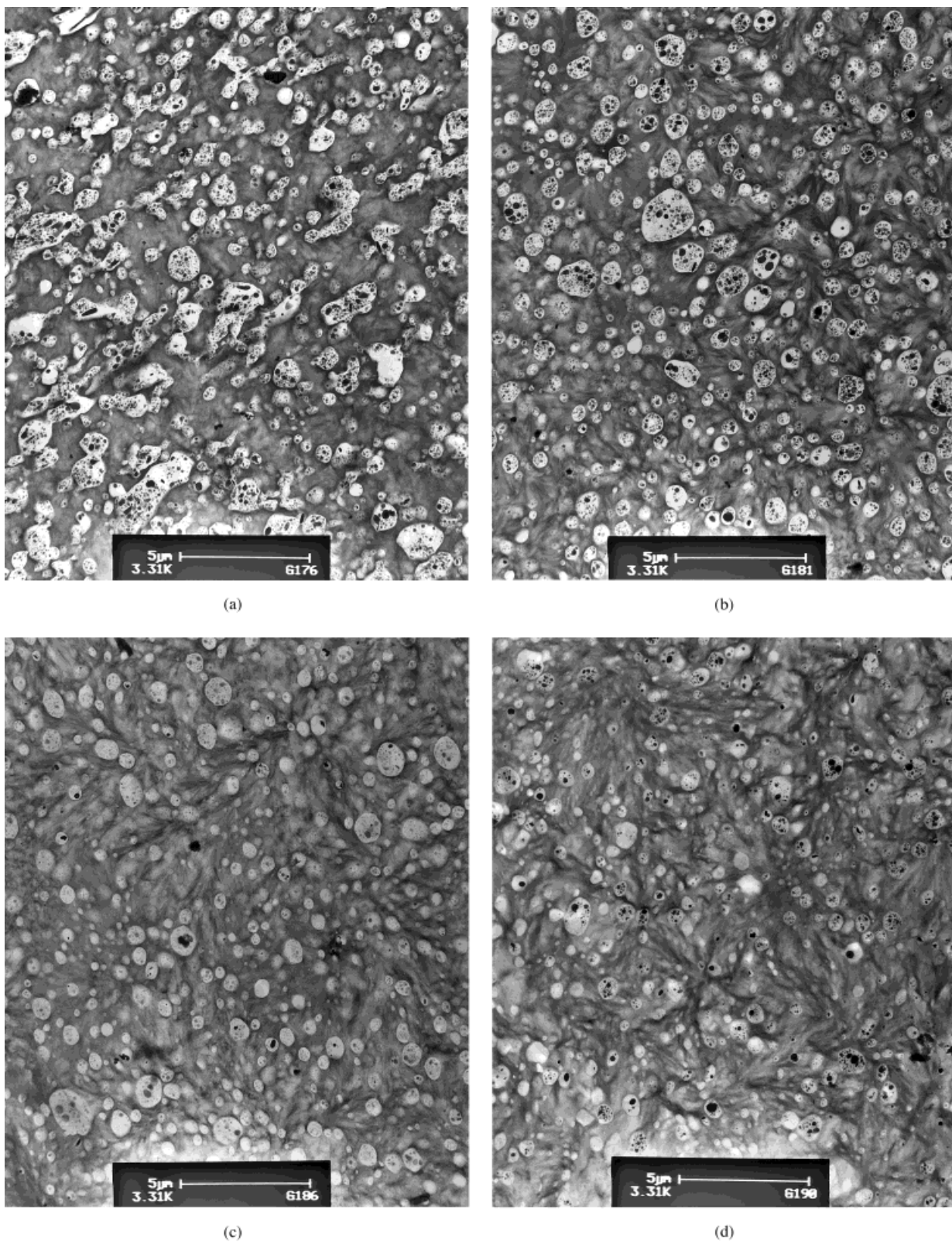


**Figure 5.** TEM micrographs of PA-6/EPM/EPM-g-MA (80/0/20a w/w/w) collected along the extruder at locations A to D (a, b, c, and d, respectively).



**Table III.** Dispersed Rubber Particle Size of PA-6/EPM/EPM-*g*-MA Blends as Determined with Electron Microscopy

| Blend       | Sampling Location | Particle Size             |                         |                              |
|-------------|-------------------|---------------------------|-------------------------|------------------------------|
|             |                   | Average ( $\mu\text{m}$ ) | Range ( $\mu\text{m}$ ) | Variance ( $\mu\text{m}^2$ ) |
| 80/20/0     | B                 | 15.8                      | 2.4–49.8                | 151.3                        |
|             | C                 | 10.3                      | 2.4–35.7                | 106.1                        |
|             | D                 | 9.0                       | 2.0–31.0                | 92.2                         |
| 80/15/5     | B                 | 2.8                       | 1.5–35.6                | 8.1                          |
|             | C                 | 2.7                       | 1.5–24.1                | 7.5                          |
|             | D                 | 2.6                       | 1.5–22.5                | 3.8                          |
| 80/10/10    | B                 | 2.4                       | 1.5–10.2                | 1.4                          |
|             | C                 | 2.4                       | 1.5–8.7                 | 1.2                          |
|             | D                 | 2.3                       | 1.5–8.6                 | 1.1                          |
| 80/5/15     | B                 | 2.3                       | 1.5–4.7                 | 0.7                          |
|             | C                 | 2.3                       | 1.5–4.8                 | 0.7                          |
|             | D                 | 2.2                       | 1.5–5.2                 | 0.7                          |
| 80/0/20a    | B                 | 0.4                       | 0.1–1.3                 | 0.06                         |
|             | C                 | 0.3                       | 0.1–0.7                 | 0.03                         |
|             | D                 | 0.3                       | 0.1–0.7                 | 0.02                         |
| 80/11.5/8.5 | B                 | 2.5                       | 1.5–10.3                | 2.0                          |
|             | C                 | 2.4                       | 1.5–7.2                 | 1.4                          |
|             | D                 | 2.2                       | 1.5–6.8                 | 0.8                          |

at the interface of the molten EPM phase and the solid PA particles.

The thermal properties (melting temperature and degree of crystallinity) of all the blends along the extruder, as determined by differential calorimetry, do not differ significantly from those of an extruded PA-6 reference ( $T_m = 223^\circ\text{C}$ ;  $\Delta H_m = 56.5 \text{ J/g}$ ). This is probably due to the high percentage of PA-6 in the blend, in combination with the low amount of copolymer formed at the interface (Table II: less than 1.1 wt.% of grafted PA relatively to PA present).

## CONCLUSIONS

This work focussed on the evolution of the grafting reaction and of the morphology development of PA-6/EPM/EPM-*g*-MA blends in a corotating twin screw extruder.

A correlation between morphology and chemical conversion could be established. Most of the chemical conversion and morphology changes occurred during melting. Since the intensive mechanical mixing induced further on in the extruder did not produce significant changes in morphology, it was postulated that the graft copolymers initially formed at the interface pro-

vide steric stabilization and avoid coalescence or break-up of the rubber particles.

The authors are grateful to DSM, The Netherlands, for the materials and technical support, to Exxon, Spain for materials and to INVOTAN for the financial support. Mrs. M. Walet (DSM Research) is gratefully acknowledged for the TEM measurements.

## REFERENCES AND NOTES

- Datta, S.; Lohse, D. *Polymeric Compatibilizers*; Hanser Publishers: New York, 1996.
- Utracki, L. A. *Encyclopaedic Dictionary of Commercial Polymer Blends*; ChemTec Publishing: Toronto, 1994.
- Majumdar, B.; Paul, D. R.; Oshinski, A. *J Polym Sci* 1997, 38, 1787.
- Lu, M.; Keskkula, H.; Paul, D. R. *J Appl Polym Sci* 1996, 59, 1467.
- Hahn, M. T.; Hertzberg, R. W.; Manson, J. A. *J Polym Sci* 1983, 18, 3551.
- Chen, D.; Kennedy, J. P. *Polym Bull* 1987, 17, 71.
- Kim, J. W.; Kim, S. C. *Polym Adv Tech* 1991, 2, 177.
- Crespy, A.; Caze, C.; Coupe, D.; Dupont, P.; Cavrot, J. P. *Polym Eng Sci* 1992, 32, 273.
- Seo, Y.; Hawang, S. S.; Kim, K. U.; Lee, J.; Hong, S. *Polymer* 1993, 34, 1667.

10. van Duin, M.; Aussems, M.; Borggreve, R. J. M. *J Polym Sci, Part A: Polym Chem* 1998, 36, 179.
11. Cartier, H.; Hu, G. H. *Proc Polyblends 97*, Boucherville, Canada, 1997.
12. Sundararaj, U.; Macosko, C. W.; Rolando, R. J.; Chan, H. T. *Polym Eng Sci* 1992, 32, 1814.
13. Sundararaj, U.; Macosko, C. W.; Nakayama, A.; Inoue, T. *Polym Eng Sci* 1995, 35, 100.
14. Sakai, T. *Adv Polym Tech* 1995, 14, 277.
15. Stephan, M.; Franzheim, O.; Rische, T.; Heidemeyer, P.; Burkhardt, U.; Kiani, A. *Adv Polym Tech* 1997, 16, 1.
16. Machado, A. V.; Covas, J. A.; van Duin, M. *J Appl Polym Sci* 1998, 71, 135.
17. Scott, C. E.; Macosko, C. W. *Int Polym Processing X*, 1995, 1, 36.
18. Retzsch, M. *Prog Polym Sci* 1988, 13, 277.